Annu. Rev. Phys. Chem. 1995. 46: 373–94

POTENTIAL ENERGY SURFACES FOR CHEMICAL REACTIONS AT SOLID SURFACES

Barbara J. Garrison and Deepak Srivastava

Department of Chemistry, 152 Davey Laboratory, The Pennsylvania State University, University Park, Pennsylvania 16802

KEY WORDS: molecular dynamics, computer simulations, gas-solid reactions, many-body potential energy surfaces, surface catalysis

ABSTRACT

Many-body potential energy surfaces (PESs) for describing atomic interactions in gas-solid and surface reaction dynamics are reviewed in this work. Initial PESs from the 1960s–1970s were restricted to a diatomic molecule interacting with a solid surface. Since the 1980s, a multitude of many-body reactive PESs, their parameterization, and their applications have been reported in the literature. Although we mention most of the PESs in general, we have chosen to describe only those that either have had general utility or have had staying power, i.e. they have been used widely by other research groups. The potentials discussed in the most detail are the Stillinger-Weber and Tersoff Si PESs, the Brenner hydrocarbon PES, and the embedded-atom method (EAM) style potentials for metals. We conclude that although these PESs have been used successfully in large-scale computer simulations, further development is needed in many-body PESs. In particular, the development of new functional forms for multicomponent reactive systems is required.

INTRODUCTION

The modeling of gas-phase chemical reactions has become highly sophisticated since the inception of the field in the 1960s. These models have been invaluable in helping chemists and other scientists to obtain a micro-

0066-426X/95/1101-0371$05.00

scopic view of the atomic motions that drive chemical reactions, as well as to predict quantitative information that could be compared to experimental data. Along came the 1970s, and chemists became interested in surface chemistry, i.e. in detailing analogous reaction pathways that occur at a two-dimensional interface. It was a natural challenge to apply computer modeling to such processes. Because microscopic simulations [classical molecular dynamics (MD) or quantum scattering] often require accurate multidimensional potential energy surfaces (PESs), the initial goal was to develop PESs that were appropriate to describe reactions at surfaces. After all, it is the quality of the PES that ultimately dictates the connection of the simulation to experimental reality.

This review encompasses the methodology associated with the construction of PESs for use in molecular dynamics simulations of chemical reactions at solid surfaces. The emphasis is on the words reaction and molecular dynamics. The fact that bond-breaking and bond-making processes are involved implicitly means that the PESs of interest are many body in nature. We review the available types of reactive many-body PESs and give examples of their applicability. Omitted because they are not reactive in nature are discussions of physisorption of a gas on a surface, unless this is a low-temperature channel for subsequent atomic adsorption or other processes; diffusion of atoms or intact molecules on surfaces; and scattering of gases using the surface as a corrugated wall. In addition, the PES must also be able to be used in MD simulations for arbitrary configurations of atoms. We have picked PESs that have had either general utility or staying power, i.e. they have been used widely by other research groups. Therefore, this is not meant to be a review of all simulations ever performed using the PESs. Finally, we believe that there is a need for more diversity in the types of PESs used for surface simulations and hope that others will be inspired to take up the challenge.

What do we mean by reactions at surfaces? First, there are reactions typical of heterogeneous catalysis on a metal surface in which the substrate atoms do not significantly move from their equilibrium positions. For example, when ethylene, C_2H_4, or acetylene, C_2H_2 plus H_2, is adsorbed on Pt{111}, the resulting species is ethylidyne, C-CH_3, as shown schematically for C_2H_4 adsorption in Figure 1 (a concise history of this saga is given in 1). This class of reaction is interesting and important, but in this particular case, the reaction mechanism is unknown (2, and references therein). There are other reactions, though, in which the surface is known to be a much more active participant. An example of this case is the etching of Si due to gas-phase F atoms, as shown in Figure 2. F atoms react with the Si substrate to make a complex interfacial regime. Ultimately a volatile species that desorbs from the surface, such as SiF_4 or Si_2F_6, is formed.

Another example is the reaction that occurs when one layer of Rh is adsorbed on a Ag surface. The Ag atoms move toward the surface, and the Rh atoms move into the second layer, as shown in Figure 3. These pictures present a visual image of how complex the overall reaction process becomes. The challenge for describing the whole manifold of events that occur with one PES can be daunting.

To develop a PES for surface reactions (or even for a gas-phase reaction), the first step is to choose a functional form with parameters and then fit the parameters to a set of data. The data may come from experiment or perhaps electronic structure calculations. This general approach works well for systems for which we have considerable intuition about the answer ahead of time. For diatomic molecules a Morse potential does reasonably well in allowing us to fit the experimental values of the bond strength, the equilibrium distance, and the vibrational frequency. Moreover, there is almost a one-to-one correspondence between the parameters and measurable quantities. As we move to systems with three or more atoms, the situation becomes more complex. First, the data are generally insufficient to fit a multitude of parameters. Second, certain properties are difficult to quantify. For example, a PES for Si should predict that the diamond lattice is more stable than all other structures. A PES for Si-F or C-H should keep the F or H atom monovalent. One cannot easily fit these conditions with any mathematical or computational algorithm; consequently the choice of the functional form becomes crucial. If the functional form is correct, then it may be possible to fold on these additional required properties of a system and numerically fit the parameters to properties that can be measured and quantified. For example, the atomic interactions in the extended materials systems are short-range bonding and long-range nonbonding interactions. With a suitable PES it is possible to study long-range strain effects in the materials through the short-range potential functions (3). Similarly with a suitable PES fitted to the available data, it might be possible to predict the mechanism for the reaction shown in Figure 1. For an unsuitable functional form, not even a very large amount of data for fitting the parameters will make the PES useful for predictive simulations.

Once the PES has been conceived and fit to known information, assessing the reliability of the result is not straightforward. Quite frankly the available experimental data for calibrating the potential for gas-surface reactions are meager when compared to those available for gas-phase reactions or even for reactions in bulk materials. Moreover, the experimental data are generally averaged over properties, such as temperature, that smear out detailed comparisons to quantities that are most sensitive to chosen parameters. So, how does one test and determine the best available potential for a particular system? The answer is unclear. The

modus operandi is to use a PES for simulations, compare the results as best as possible with experimental data, and go forth. We offer another subjective test from Jerry Tersoff, a constructor of PESs for group IV elements.[1] His test comes in two parts. First, has the person who constructed the potential subsequently refined the potential based on initial simulations? This gives some indication of whether the developer of the potential is committed to finding a good potential. Second, has the potential been used by other researchers for simulations of phenomena for which the potential was not designed? This question refers to simulations in which the PES is used as is and not to those in which someone does a little tweaking of the potential parameters and says they have a new PES. Only a handful of PESs pass the Tersoff Test.

We have been active users (and only dilettante constructors) of empirical PESs for reactions at surfaces for many years. They are critical input for our simulations. They have allowed us to model many phenomena for which we have obtained insight that is useful for interpretation of experimental data. In constructing a list of the types of potentials for this article, it is apparent (*a*) that we are still a long way from modeling all possible reaction types and (*b*) that there has been a slowdown in the development of new potential forms. It is clear to us that computer modeling of realistic systems will continue to grow. What the field needs are some new ideas in constructing empirical PESs.

POTENTIAL OPTIONS, OR OPTIONS FOR POTENTIALS

There are three main groups of empirical PESs, which are discussed below. The first is the London-Eyring-Polanyi-Sato (LEPS) form because historically this approach was tried first. The development of PESs for group IV elements and metals then occurred almost simultaneously. Of these we choose to discuss the group IV elements first because to us these are more chemical in nature.

The LEPS Approach, or Our Heritage from Gas-Phase PESs

Following the success of Polyani in using LEPS potentials (4) to describe energy transfer in atom + diatom reactions in general (5) and of Muckerman to investigate the $F + H_2 \rightarrow FH + H$ reaction in particular (6–8), it is not surprising that the LEPS approach was quickly transported to reactions at surfaces. The seminal work in this area was by McCreery & Wolken (9). They examined the reaction of H_2 with a W{001} surface in

[1] J Tersoff, private communication, December 6, 1994. He is the person that relayed these questions to BJG. Others may, in fact, use the same criteria.

which there are three constituents: two H atoms and the W surface. Simplistically, the H_2 interaction within the LEPS prescription is described by bonding and antibonding states that include the adjustable Sato parameter.[2] They assumed that the surface is periodic and rigid. (Assuming that the massive W atoms remain stationary while the light H atoms collide with them is not an unreasonable approximation.) The H-W interaction is a Morse potential in which the well depth, equilibrium height above the surface, and screening length are all periodic functions of the lateral position on the surface. In contrast to the following sections in which the basic equations for the main potentials are given, in the LEPS approach there are too many equations and too many parameters to be provided in this limited space. We believe that this, in fact, is one of the limitations of the LEPS approach for gas-surface reactions.

The LEPS potential is capable of describing both molecularly adsorbed H_2 and two H atoms bound on the surface. Moreover, the binding energy of each species depends on the lateral position. The Sato parameter allows flexibility whereby one can tune the relative energies of the molecularly adsorbed state vs atomically adsorbed state and also the nature of the barrier for desorption.

McCreery & Wolken went on to perform molecular dynamics simulations in order to investigate a number of processes, including molecular scattering (10), adsorption of H_2 from the gas phase (11), molecular desorption of H_2 from two H atoms on the surface (12, 13), and the Eley-Rideal pickup of one H atom on the surface by an incoming H atom (14).

The next workers to use the LEPS potential were Gelb & Cardillo, who examined the dissociation dynamics of H_2 adsorbing on the rigid low-index faces of Cu (15). Andeev et al fit a LEPS H_2-Ni$\{001\}$ potential based on energetics, bond lengths, and frequencies calculated by electronic structure techniques (16). McCreery & Wolken incorporated a modification to correct for moving solid atoms in their H_2-W$\{001\}$ potential (17). Gregory et al included explicit Cu atom positions in their LEPS potential in order to investigate binding to stepped surfaces (18), and Purvis & Wolken included explicit atoms in order to examine amorphous surfaces (19). In 1980 Tully investigated the Eley-Rideal reaction in which an incident gas-phase O atom reacts with a C atom adsorbed on a Pt$\{111\}$ surface to yield a gaseous CO molecule (20).[3] The potential describes

[2] There are different phraseologies used to describe LEPS potentials and also the related diatomics in molecules (DIM) approach. We have chosen one phraseology for this entire section rather than use the words of each worker.

[3] This calculation was inspired by exquisite experiments by Wharton's group at the University of Chicago. To date the experimental data have never been published.

surface atomic O and C adsorption sites and also molecular sites for the CO. The Pt atoms vibrate around their equilibrium positions and the gas atom–Pt interaction includes an explicit pair-wise sum over the metal atom positions. Potentials for H_2 dissociation on Pt{111} (21, 22) and O_2 on Ni{001} were developed (23). Lee & DePristo modified the LEPS prescription to include terms that are based on effective medium theory to fit H_2-Ni and H_2-Cu potentials in order to examine dissociation dynamics (24, 25), and Truong et al modified these potentials (26). Kara & DePristo later developed an N_2-W{110} potential (27).

As variants on a theme, McCreery & Wolken extended the LEPS model to three H atoms plus the W{001} surface (28). Lin & Garrison studied three O atoms on a Ag{110} surface (29). These workers were able to fit the available experimental data and to examine adsorption probabilities. Olson & Garrison applied a similar approach for nonadiabatic charge exchange reactions at surfaces (30).

The LEPS potential has been used primarily for diatomic molecules interacting with metal surfaces. The Sato parameter makes it possible to adjust energetics of molecular and atomic adsorption sites and activation barriers. Most of the time, though, we do not know from experiment what these values are, so it becomes challenging to know when one is converging on the right potential. In 1980 Tully clearly assessed the situation (20):

> The available experimental information is by no means sufficient to prescribe the entire multidimensional potential energy hypersurface. Thus the interaction potential employed here is very uncertain. Nevertheless, the major qualitative conclusions of this study—that the product CO molecule escapes quickly from the surface and carries considerable internal excitation—are unaffected by substantial alterations of the interaction potential.

Moreover, after our own work on the O-Ag system (29), we reached additional conclusions about using LEPS potentials for reactions at surfaces. First, the potential becomes computationally intensive for several gas atoms. The three–gas atom potential involves diagonalizing a 5×5 matrix for each potential evaluation and then requires several matrix multiplications to get the forces for the MD simulation. Second, to go from three gas atoms to four atoms would require redeveloping the formulas rather than extending the "Do Loop" by one.

In some sense the LEPS potential formulation of McCreery & Wolken passes the Tersoff Test, but the individual potentials do not. Functional forms are needed that better describe the chemistry of interest and that have fewer parameters. In the mid-1980s this situation started to occur in two directions—for Si and for metals. We have arbitrarily chosen to discuss Si and other group IV elements first.

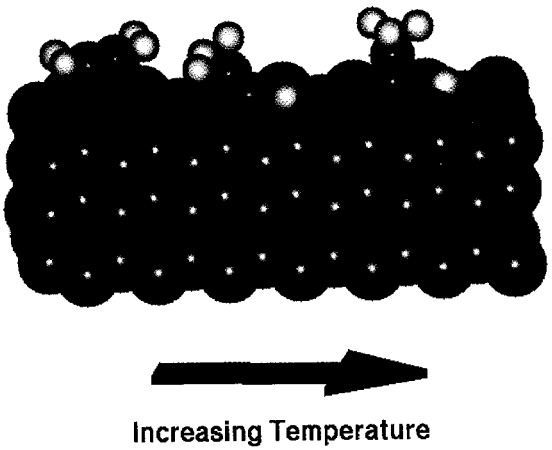

Figure 1 Schematic representation of the conversion of C_2H_4 to C_2H_3 on a Pt{111} surface. The precise reaction mechanism is unknown (2). The Pt atoms are depicted in green, the C atoms in pink, and the H atoms in yellow. This picture is taken from the work of Taylor & Garrison (RS Taylor & BJ Garrison, unpublished data), who modeled the kilo electron volt particle bombardment of the preadsorbed C_2H_3 on Pt{111} in which the EAM potential is used for the Pt interaction (112), Brenner's potential for the hydrocarbon interactions (35, 74), and a blend of potentials for the Pt-C interactions (79).

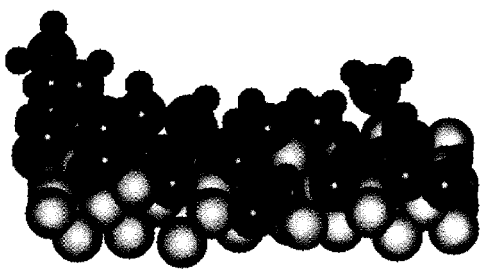

Figure 2 Etch region of a Si substrate from a MD simulation by Schoolcraft & Garrison (44). The potential used is from Stillinger & Weber (31, 36–38). The top three layers of the crystal at the end of the simulation are depicted. Yellow spheres represent nonfluorinated silicon atoms, green spheres represent monofluorinated silicon atoms, orchid spheres represent difluorinated silicon atoms, and red spheres represent trifluorinated silicon atoms. Small blue spheres represent the fluorine atoms. The exposed -SiF_3 groups are ripe for a reaction with another incoming F atom to form SiF_4.

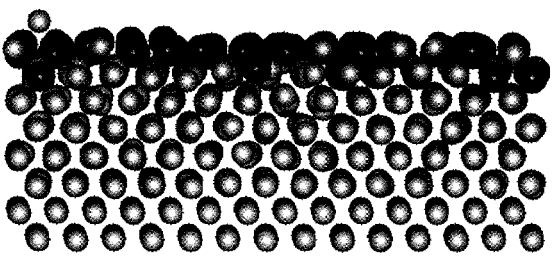

Figure 3 Final positions after 15 ps of Rh and Ag atoms after annealing at 600 K a configuration of 0.5 monolayer of Rh on Ag{001}. The simulation is from DePristo and coworkers (133, 134) using the MD–MC-CEM potentials (131). The Ag atoms are depicted in blue, and the Rh atoms in maroon.

Group IV Elements

In our opinion it is the Si potential by Stillinger & Weber (SW) (31) that signaled the start of the explosion of potentials for diamond lattices (e.g. Si, GaAs, Ge, and C). To be historically correct, the first Si potential to appear in the literature was developed by Pearson et al (32) and is based on the Axilrod-Teller three-body prescription (33). It is the SW potential, though, that has gained the most popularity. In contrast to the LEPS formulation, the potentials discussed below are cast in a form such that one can easily consider an arbitrary number of atoms. Describing the bonding in Si requires that the potential (functional form and parameters) predict that the diamond lattice (each atom has four neighbors in a tetrahedral arrangement) be more stable than all other configurations. This is a challenge because simple potentials like a pair-wise sum of Morse or Lennard-Jones interactions predict that a close-packed structure, such as a face-centered-cubic (fcc) metal with 12 nearest neighbors, is most stable.

From our perspective of the many different functional forms proposed for Si, two PESs have continued to be used by a large number of different groups, i.e. they have passed the Tersoff Test. These potentials are by Stillinger & Weber (31) and Tersoff (34). It is unclear whether they are the best potentials. We believe their staying power has been due to two factors: (*a*) the relatively simple functional forms needed for computer coding and (*b*) the fact that they have been extended to elements besides Si. One important adaptation of the Tersoff potential is by Brenner in which he has constructed a potential for reactions among hydrocarbon molecules and diamond surfaces (35). This potential is also being used in simulations of reactions by various researchers. We discuss these three potentials and briefly mention the others.

The Stillinger & Weber Potential

The SW potential (31) was originally developed to describe Si interactions and was later adapted for F_2 (36) and Si-F (37, 38) bonding interactions. This potential is based on the expansion of the total interaction potential in n-body terms as

$$V(\mathbf{r}_1, \mathbf{r}_2, \ldots \mathbf{r}_n) = \Sigma_i \Sigma_{j>i} V_2(r_{ij}) + \Sigma_i \Sigma_{j>i} \Sigma_{k>j} V_3(r_{ij}, r_{ik}, r_{jk}) + \ldots, \qquad 1.$$

where V_2 is the two-body term and V_3 is the three-body term, and four-body terms and higher are omitted. In the SW work the following form is used for V_2:

$$V_2(r_{ij}) = A(Br_{ij}^{-p} - r_{ij}^{-q}) \exp[c/(r_{ij} - r_c)], \qquad 2.$$

where A, B, c, p, and q are parameters. The first term in Equation 2 has a

Lennard-Jones form, and the second term is a cutoff function that smoothly terminates the potential at a distance r_c. This cutoff makes the computations more tractable than an infinite ranged potential, as there are fewer interactions to evaluate. The Si three-body term is written as

$$V_3 = h(r_{ij}, r_{ik}, \theta_{jik}) + h(r_{ji}, r_{jk}, \theta_{ijk}) + h(r_{ki}, r_{kj}, \theta_{ikj}), \quad 3.$$

where

$$h(r_{ij}, r_{ik}, \theta_{jik}) = \lambda \exp[\gamma/(r_{ij} - r_c) + \gamma/(r_{ik} - r_c)] \{[\cos(\theta_{jik}) - \beta]^2\}, \quad 4.$$

with λ, γ, and β as parameters and θ_{jik} the angle centered on atom i. The first factor in Equation 4 is for ensuring a smooth cutoff as the participating bonds are stretched. There are many ways to describe the two- and three-body interactions, but the simplest is that V_2 is a bond stretch and V_3 is an angle bend in the SW potential. The V_3 term is designed to maintain the tetrahedral angle of the Si crystal structure (diamond lattice) because the value of β is $\cos(109.47^\circ)$. This potential describes reactions, i.e. Si atoms can be added and subtracted from the surface and the potential and forces remain continuous and smooth.

For determining the Si-F interactions, SW modified the functional forms somewhat and then fit the parameters in V_2 and V_3 to experimental data such as the lattice and the elastic constants and the melting temperature of Si, the energetics and geometries of F_2 and SiF_x molecules, and whatever else they could find. The three-body terms are constructed so that F is always monovalent.

SW published MD simulations with all their potentials, examining the melting and freezing of Si (31), the dissociation of F_2 in a condensed state of F_2 molecules (36), and the fluorination of the Si{001}(2×1) dimerized surface by gas-phase F_2 molecules (37, 38). Grabow and coworkers built a special parallel computer in order to model the motion of a crystal-melt interface of Si with the SW potential (39, 40). Broughton & Li used MD simulations to map out the phase diagram of liquid, crystal, and amorphous Si (41). Uttormark et al developed a method for combining nonequilibrium MD simulations with Markovian data analysis techniques for studying both the growth and dissolution of crystalline embryos in the liquid phase (42). Schoolcraft & Garrison used the Si-F potential to examine F atom adsorption onto the Si{001}(2×1) surface (43) and also modeled the reactive etching of Si in which Si_xF_y species spontaneously desorbed from the surface (44). A snapshot of the surface from this simulation is shown in Figure 2.

This potential has gained enormous popularity and clearly passes the

Tersoff Test, but it does have certain limitations.[4] First, the three-body term defines one equilibrium configuration, in this case a tetrahedral geometry. How one would extend the potential to an element such as C, which can have equilibrium angles of 180°, 120°, and 109.47°, is not obvious. Second, with this functional form it is impossible to fit the cohesive energy and bond length of both bulk silicon and Si_2. SW chose to fit the bulk rather than the diatomic molecule properties. (In fact, in all of the empirical potentials a choice has been made as to which properties are more important to fit than others.) Third, the energy to remove an F atom from gas-phase SiF_x species varies monotonically from 5.72 eV for SiF to 6.46 eV for SiF_4 with this potential. The experimental quantities, however, oscillate, having values of 5.72, 6.72, 5.33, and 6.93 eV for $x = 1$–4, respectively (45). These comments are not meant as criticisms but rather as statements of the difficulty of finding a perfect functional form to describe chemical reactions at surfaces.

Investigators have adapted this functional form to other elements. Ding & Andersen rescaled the potential for a Ge version (46), as did Roland & Gilmer (47); Weakliem et al reparameterized the Si-F portion of the potential based on ab initio calculations for surface adsorption but still did not make the Si-F bond strengths oscillate (48, 49); Feil et al developed a Si-Cl version (50); and Wu et al developed a Si-H parameterization (51). Feurston & Garofalini have used a similar three-body term for vitreous silica (52). Mahon et al fit a C version based on ab initio calculations (53).

The Tersoff-Abell Potential

In determining his potential for group IV elements (Si, Ge, and C), Tersoff attacked the problem quite differently (34). His potential does not build on the expansion in many-body terms but is in actuality an explicit three-body potential with implicit many-body interactions. He writes the interaction potential as

$$V(\mathbf{r}_1, \mathbf{r}_2, \ldots \mathbf{r}_n) = \tfrac{1}{2}\Sigma_i\Sigma_j[V_R(r_{ij}) - b_{ij}V_A(r_{ij})], \qquad 5.$$

where V_R and V_A are the repulsive and attractive portions of the pair-like Morse interaction. The difference between this potential and a pair potential is that the coefficient of the attractive term, b_{ij}, depends on the

[4] In fact, there is only one published version of the SW Si potential. This is a credit to Stillinger & Weber. They performed lots of simulations and refined the PES before publishing it. Moreover, to our knowledge no one has reparameterized it for Si.

neighbors of atom i. The parameter b_{ij} arises from a bond order concept taken from Abell (54). Tersoff assumes that

$$b_{ij} = (1+\beta^n \zeta_{ij}^n)^{-1/2n}, \quad 6.$$

with

$$\zeta_{ij} = \Sigma_{k \neq i,j} g(\theta_{ijk}), \quad 7.$$

and

$$g(\theta) = 1 + c^2/d^2 - c^2/(d^2 + (h - \cos\theta)^2). \quad 8.$$

In these equations β, n, c, d, and h are parameters. The angular dependence is in the b_{ij} term but not in a straightforward manner. This potential is still a functional form with parameters that must be fit to experimental data. The Tersoff functional form allows one to fit Si_2 energetics as well as bulk Si properties, which is impossible with the SW potential. There are cutoff functions in the Tersoff potential that allow for speedier computations, but these are not explicitly shown in Equations 5 and 7 in order to more clearly illuminate the functional forms.

The flexibility of this functional form is that there can be local minima for several different coordinations, and it allows low-coordination configurations to be more stable than high-coordination ones. Because of this functional form, Tersoff could fit the parameters to the energy and bond lengths of bulk Si, Si_2, and calculated energetics of simple cubic and fcc structures of Si (34). This first potential, though, has a structural minima that is not the diamond lattice that resulted in Tersoff's second parameterization (55) and Dodson's work (56). Herein lies a big challenge to developing a potential for a diamond (really any nonclosed packed) lattice: How does one make absolutely sure that the desired structure is the global minimum of the PES? Tersoff fit a third version in which the elastic constants of Si and properties of SiC were better described (57), but to do this he had to sacrifice the fit with the nondiamond structures of Si. The cohesive energy per atom and per bond for the Si potential along with the energetics from the electronic structure calculations (58, 59) for the various forms of Si are shown in Figure 4.[5] The cohesive energy per bond decreases as the number of neighbors increases as per the concept within the model. The energy per atom, however, minimizes at a coordination of four—the structure of bulk Si.

A sampling of the simulations using Tersoff's potential is given below. Kitabatake et al performed MD simulations of 10 eV Si irradiation of

[5] Most workers currently use Tersoff's third Si potential, which is given in Reference 57.

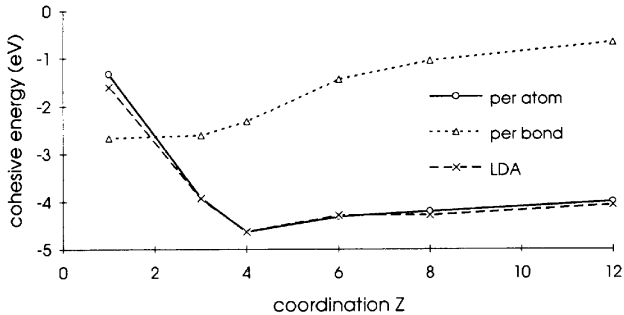

Figure 4 Cohesive energies for Si (57). The points correspond to the following structures: dimer, graphite, diamond, simple cubic, bcc, and fcc. Also shown are the local density approximation electronic structure values from Yin & Cohen (58, 59).

Si substrates in order to examine defect structures produced (60, 61). Kitabatake and coworkers examined the mechanism of SiC heteroepitaxial growth by carbonization of the Si{001} surface (62). We identified the anisotropic spread of surface dimer openings in the initial stages of epitaxial growth on Si{001} via MD simulations (63). Kelires & Tersoff investigated equilibrium structures of SiGe alloys (64).

As stated above, the strength of the Tersoff form is that many different binding configurations can all be local minima, a feature that Brenner exploits in his hydrocarbon potential. There is one serious problem: the cutoff function. It makes the potential (and forces) go quickly to zero as the cutoff distance is approached. If the energetics and/or dynamics of interest fall in this distance regime, one must use caution.

Tersoff fit three versions of the Si (34, 55, 57) PES as well as a Ge and C PES (65). Dodson reparameterized the Si potential (56), and Wang & Rockett reparameterized it again (66). Bolding & Andersen fit a similar potential for Si in which they concentrated on fitting cluster energetics (67). Smith developed a GaAs potential (68). Brenner adapted the functional form for C, H, and O interactions, with each element treated separately (69). Murty & Atwater adapted the form for Si-H interactions (70). There is another family of potentials that are similar to the Tersoff potential but contain a parameter that is an effective coordination number that does not change during the course of a simulation, so the potentials cannot be used in a general MD simulation in which the number of neighboring atoms might change (71–73).

The Brenner Hydrocarbon Potential

In a tour de force, Brenner and coworkers developed a potential for C-H interactions because they were interested in simulating chemical vapor

deposition of diamond films from a gaseous mixture of hydrocarbon atoms, molecules, and radicals (35, 74). This potential has many parameters, but a plethora of experimental data is available for energies and geometries of small hydrocarbon molecules and radicals as well as the bulk diamond and graphite phases. In this prescription, the bond order term b_{ij} in Equation 5 is averaged over the ij and ji components, and a term is incorporated that counts the number of H and C neighbors along with their conjugation. An important feature of this potential is that it determines from the atomic coordinates whether a C atom should have a tetrahedral environment indicative of sp^3 hybridization, a planar geometry indicative of sp^2 hybridization, or a linear configuration as in acetylene, HCCH. The atomic positions of the hydrocarbon molecules shown in Figure 1 are determined from this potential. The gas-phase ethylene, C_2H_4, is planar, whereas each carbon in ethylidyne, C_2H_3, has a tetrahedral configuration.

This potential is attracting users because organic reactions in complex environments can be modeled. Brenner and coworkers have modeled a number of phenomena ranging from H abstraction from a H-terminated diamond surface (75) to collision and subsequent reactions of buckminsterfullerene with a diamond surface (76) to tribochemistry of two hydrocarbon surfaces (77). We predicted the mechanism for insertion of CH_2 into a surface dimer on the diamond $\{001\}(2 \times 1)$H surface from MD simulations (78) and have modeled kilo electron volt particle bombardment of organic thin films on metal surfaces (79–81). Raff, Thompson, and coworkers have examined the adsorption, abstraction, and reaction of a number of small molecules on various diamond surfaces (82–84). These are simulations in which the experimental reaction products are generally unknown, and certainly no data exist to support the proposed mechanisms. The availability of an empirical potential that allows one to explore for possible reaction paths is a great advantage. In addition to the sharp cutoff function, the serious limitation here is that the long-ranged van der Waals interactions are not included. As interest grows in modeling biological systems (85) or even self-assembled monolayers on surfaces (86), it would be nice to have both the long-range and short-range interactions in one functional form.

Other Potentials for Group IV Elements

There are a number of other Si potentials in the literature. Shortly after the SW potential appeared, there was one by Biswas & Hamann (87) and a revision by the same developers (88). They also constructed a Si-H PES (89). As with the SW potential, Biswas & Hamann (90) expand the potential in two- and three-body terms. The three-body term is then expanded

in Legendre polynomials. This potential is long-ranged and extends to 10 Å, making it computationally expensive. Brenner & Garrison developed a dissociative valence force field potential for Si (90) based on the Keating model of vibrational motion (91). Baskes developed a modified embedded-atom method (MEAM) potential for Si (92). Kaxiras & Pandey constructed a two- and three-body potential refined to describe a diffusion path in bulk Si as well as the other properties such as cohesive energy (93). Mistriotis et al included two-, three-, and four-body terms in their potential in order to describe cluster energetics (94). Tiller and coworkers have fit their potential of Axilrod-Teller (33) form for a number of group III-V compounds in addition to the group IV elements (32, 95–99). Chelikowsky, Phillips, and coworkers developed a potential for Si in which they fit both high-coordinated configurations like fcc and body-centered-cubic (bcc) phases as well as cluster energetics (100, 101). Chelikowsky later made a C version of the potential (102). Murrell & Mottram have developed a general approach for PESs for atomic systems based on a two- and three-body expansion in normal-mode coordinates (103). Murrell et al have applied this methodology and developed PESs for the group IV elements of C, Si, Ge, and Sn (104–106).

Balamane et al have published an extensive comparative study (107) of their own Si potential (32) along with potentials of Tersoff (57), Stillinger & Weber (31), Biswas & Hamann (87), and Dodson (56). They also comment upon the Kaxiras & Pandey (93), Mistriotis et al (94), Khor & Das Sarma (71–73), Bolding & Andersen (67), Chelikowsky et al (100, 101), and MEAM Si potentials (92). The review emphasizes how well each of the potentials performs at calculating various quantities that can be compared to experimental data or to electronic structure calculations. Cook & Clancy (108) examine the melting behavior of the Tersoff (57) and MEAM Si and Ge potentials (92).

Metal Potentials

There are two basic reasons that one must go beyond pair potentials in order to describe the interactions in metals. First, the energies are not pairwise additive. Consequently it is impossible to simultaneously describe both the bulk cohesive energy and the energetics of lower-coordination configurations like a vacancy or a surface. Second, pair potentials predict that the elastic constants C_{12} and C_{44} are equal, a condition that is invalid for almost any metal.

There are three main metal crystal structures: fcc, bcc, and hexagonal closest packed (hcp) (109). The fcc and ideal hcp crystals are similar in that they are both close-packed structures with an atom having 12 nearest

neighbors (albeit arranged differently) and 6 second-nearest neighbors. The differences in number of atoms do not appear until the third neighbor shell. Thus for any potential with spherical symmetry, such as the EAM, the energy differences between fcc and hcp will be small. The bcc crystal is more open, with eight first-nearest and six second-nearest neighbors. The consequence of this is that it is easiest to find a PES that predicts a fcc structure to be most stable. Thus we discuss the fcc PES first. The bcc and hcp PES are discussed thereafter.

fcc Potentials

The ability to model fcc metals in simulations with a many-body potential started with a paper by Daw & Baskes in 1983 in which they examined hydrogen embrittlement in Ni (110) with an extension to H in Pd (111) by the EAM. In 1986 Foiles et al developed EAM potentials for all six group VIII elements (112) and, moreover, made their computer code for simulations available for others to use. The EAM potential is based on quasiatom (113) and effective medium (114, 115) theories but is implemented as an empirical functional form in which the parameters are fit to experimental data. The energy of the ith atom is written as a sum of the energy to embed the atom in an electron density and a two-body component as

$$E_i = \Sigma_i F(\rho_i) + \tfrac{1}{2}\Sigma_i \Sigma_j \Phi_{ij}(r_{ij}), \qquad 9.$$

where the density, ρ_i, is expressed as a sum of atomic densities, ρ_{at},

$$\rho_i = \Sigma_j \rho_{at}(r_{ij}). \qquad 10.$$

Here r_{ij} is the distance between atoms i and j, F is the embedding energy, and Φ_{ij} represents electrostatic interactions between atoms i and j. The partitioning between the pair term Φ_{ij} and the embedding energy $F(\rho_i)$ is not unique. These workers have chosen to express Φ_{ij} as purely repulsive, and thus $F(\rho_i)$ is negative for geometries of chemical interest. Φ_{ij} is expressed as $Z_i(r)^* Z_j(r)/r$; the Z_i is an effective charge.

Like all functional forms with parameters, the parameters must be fit to a set of experimental data. In this case the relevant quantities include the cohesive energy, the lattice and elastic constants, vacancy formation energies, and mixing energies for alloys. To effectively do this, though, one must choose functional forms for $Z(r)$ and $F(\rho)$. Foiles et al (112) chose to express $Z(r)$ as a functional form with parameters, to use ρ_{at} from electronic structure tables, and to tabulate $F(\rho)$ as a function of ρ by fitting to the universal equation of state of Rose et al (116). This equation of

state gives the cohesive energy of a crystal as a function of the lattice constant for homogeneous expansions and contractions of the system.

The functional form for the EAM potential is transferable to alloys of these elements. The pair term, Φ, is an explicit function of each atom's effective charge, Z(r). The density, ρ, is determined from a sum over atomic densities regardless of the atomic origin, and the embedding energy, $F(\rho)$, is characteristic of the atom of interest and not the source of the surrounding electron density. Given the dynamic range of possible systems that can be modeled, it is not surprising that these EAM potentials (112) pass the Tersoff Test with flying colors.

As with all the empirical forms, there are some limitations of the EAM method. The atomic densities, ρ_{at}, used are spherical, as is Φ. This almost automatically means that the lowest-energy structure will be closed-packed like the fcc or maybe the hcp lattice. The lowest-energy configuration of a metal trimer is an equilateral triangle, and the lowest-energy configuration of a metal tetramer is a tetrahedron. These predictions are not necessarily correct. In addition, one would like to develop EAM potentials for other elements. Baskes (92, 117) and Baskes & Johnson (118) have, in fact, started on this. There are mathematical and conceptual problems though. For example, if one takes oxygen on almost any transition metal, there is charge transfer from the metal to the oxygen, which makes the oxygen negatively charged. One now needs to subtract rather than add electron density to the surface metal atoms.

One example of the use of the EAM potentials is an energetic study of the {110} surfaces of the Group VIII metals. The bulk-terminated surface consists of closed-packed rows of atoms in one direction with these rows forming valleys and ridges in the opposite direction. There is one possible reconstruction, dubbed the missing-row model, in which every other ridge row is missing. This creates a larger valley and ridge structure. The EAM potential correctly predicts the experimental observations that the missing-row reconstruction is more stable for Pt and Au, whereas the bulk-terminated structure is more stable for the other four elements (119).

Other similar methods have also been developed, and different parameterizations of the EAM made. Voter developed EAM potentials for Al, Ni (120), and Ag (121) in which he assumed that the pair term is a Morse potential. He also allowed the atomic densities to be functional forms with parameters to fit. Chen et al constructed an alloy potential for Ni_3Al (122). One nicety of the Voter EAM potentials is that he fit some of the dimer properties as well as the bulk properties.[6] The Sandia EAM

[6] Art Voter also fit the Group VIII plus Rh interactions, but he never published them. These are now in a 1993 Los Alamos Unclassified Report (LA-UR-93-3901).

potentials (112) tend to overbind the dimers. Ting et al fit EAM potentials for Ni, Pd, Pt, and Au but did not use alloy information (123). We fit a Rh EAM potential in order to examine kilo electron volt particle bombardment of Rh{111} (124).

Ercolessi et al developed a similar potential, which they called the glue model, and examined the reconstruction of Au{001} (125). Lim et al fit a Pb potential in order to examine small Pb aggregates (126). Johnson developed an EAM style potential for fcc metals (127) and their alloys (128). Jacobsen et al put the EAM empirical potential on a firmer theoretical basis (129).

An alternative approach for describing fcc metal interactions is the work of DePristo and coworkers (130, 131). Historically they were developing corrected effective medium (CEM) theory as a method for electronic structure calculations (131). Desiring a function for the energy and forces that could be used in MD and Monte Carlo (MC) simulations, they turned from ab initio embedding functions to empirical embedding functions. The interaction energy, ΔE, of the entire system in these MD–MC-CEM potentials is written as

$$\Delta E = \Sigma \Delta F_i(\mathrm{A}_i; n_i) + \tfrac{1}{2}\Sigma_i \Sigma_j V_c(A_i, A_j), \qquad 11.$$

where the set of atoms is $\{A_i,\ i = 1,\ N\}$. The term ΔF_i is an empirical function designated to ensure that the expression describes the properties of the atom in bulk and diatomic environments. The last term, V_c, is the coulombic interaction between atoms A_i and A_j. This term is calculated from first principles and is not part of the fitting procedure. The embedding energies for the group VIII plus Rh elements are fit to bulk properties as well as dimer properties (132). As mentioned above, the Sandia EAM potentials are not fit to the dimer properties. Another feature of the MD–MC-CEM potential is that it obeys reasonable coulombic behavior at small internuclear separations. The added features of correct dimer energetics and repulsive interactions at small internuclear separations is important to our own work as we model kilo electron volt particle bombardment of solids in which atoms and clusters eject (132a).

A simulation of a surface reaction has been performed using the MD–MC-CEM potential. DePristo and coworkers adsorbed a half monolayer of Rh atoms on a Ag{001} surface (133, 134). They then heated the surface and within 10 ps at 600 K approximately 10% of the Rh atoms had exchanged with Ag atoms, as shown in Figure 3. These results are in agreement with experimental data showing that a sandwich compound results when Ag is dosed with Rh (135).

Reviews of EAM style potentials exist, including one by Raeker & DePristo (131) and one by Daw et al (136).

bcc and hcp Potentials

The development of bcc and hcp potentials based on the effective medium formalism occurred at about the same time as the development of the EAM fcc potentials. The bcc and hcp potentials have not, however, reached the same level of popularity for use in MD simulations as the EAM fcc potentials. It is not completely clear why this has happened. Perhaps it is due to the difficulty in obtaining bcc or hcp potentials that successfully meet all the criteria of energy stability and proper elastic constants. In addition many of the developers of the potentials have been primarily concerned with energetics of systems and not the dynamics.

Shortly after the EAM potential was published, Finnis & Sinclair developed a similar potential for five bcc metals (137). They took $F(\rho) \propto -\sqrt{\rho}$ from tight-binding theory and analytically fit the parameters to elastic constants and cohesive energies. Their potential has been modified by Rebonato et al (138), Ackland & Thetford (139), and Eridon & Rao (140). Johnson & Oh developed an analytic EAM method for bcc crystals (141), and Carlsson fit a bcc W PES (142). Murrell and coworkers have developed bcc potentials (143) based on their normal-mode expansion of the three-body term (103). Potentials for hcp metals have been developed by Bacon (144), Oh & Johnson (145, 146), and Igarashi et al (147). A proceedings volume from several years ago provides examples of the use of some of these potentials (148).

The huge popularity of the EAM potential convinced the authors to develop it for other materials. The first such endeavor was for Si by Baskes (92). To assure that the open diamond lattice is more stable than closed-packed structures, Baskes included an angular dependent term in the density. Baskes et al extended the MEAM to Si and Ge (149). Adams & Foiles fit a bcc vanadium potential (150). Considering only the first-neighbor interactions, Baskes fit MEAM potentials for ten fcc, ten bcc, three diamond cubic, and three gaseous materials (117). Some of these potentials, including the bcc and diamond lattices, are not global minima (see Table VI of Reference 117). Baskes & Johnson then went on to fit 18 hcp elements (118).

Combinations and Others

It is not surprising that workers have tried to combine various potentials for systems with different types of elements. Brenner showed that the EAM and Tersoff approaches are equivalent if only nearest-neighbor interactions are included (151). Ashu et al used this idea to construct a Si-

Ni potential in order to examine nickel silicides (152). Truong and co-workers have combined the DIM and EAM methods for a H-Ni PES (153, 154). Taylor & Garrison have blended the Brenner CH potential with the EAM in order to investigate the kilo electron volt particle bombardment of small hydrocarbon molecules on a Pt surface (79–81). Kress & Voter developed the rotated second-moment approximation to describe directional bonding (155).

CHALLENGES AND THE FUTURE

There have been some wonderfully successful PESs. These potentials and many others have been used in MD simulations for examining processes that occur at a surface and in the bulk. Balamane et al (107) summarize the situation for Si, but this applies to all the PESs:

> In conclusion, none of the potentials considered in this work appear to be superior to the others. Each has its strengths and limitations. None is totally transferable. Despite their shortcomings, we do believe that some of these potentials will be useful in large-scale simulations of materials-related problems as they can give insights into phenomena which are otherwise intractable to investigate either experimentally or with first principles methods.

We concur with their assessment. Empirical PESs have allowed us to model systems and gain new understanding about the physical phenomena involved.

The issue to address is what else would one like in a PES for reactions at surfaces, and here we get to dream. A good example is the reaction shown in Figure 1 for the formation of ethylidyne, C_2H_3, on Pt{111}. We have performed MD simulations of kilo electron volt particle bombardment for this system (79–81, 156, 157). Given an initial arrangement of C_2H_3 molecules on the surface, we can reasonably model the ejection, fragmentation, and reaction of the C_2H_3 molecules and the ejection and formation of dimers and trimers of the Pt metal.[7] What cannot be modeled is the reaction of ethylene, C_2H_4, to form adsorbed C_2H_3. Ideally one would like a PES that would predict the reaction mechanism. Modeling the ejection and stability of PtC_xH_y species is impossible with current potentials, yet these types of molecules are abundant in experimental spectra. Because the Brenner hydrocarbon potential does not include long-range interactions, predicting the relative stability of a quarter monolayer coverage vs a half monolayer coverage is not possible. [One could switch

[7] In these studies we did use the EAM potentials that overbind the dimers and trimers, but in principle another metal potential could be used that describes these energetics better.

functional forms and use molecular mechanics type potentials (158), but then one could not model reactions.] Finally what we would like to investigate next is the ejection of peptides from surfaces (159). To answer the question at the beginning of this paragraph, we want a PES for reactions among many different elements—in this case metal atoms along with C, H, N, O, and S.

One issue to address is the work that has followed Car & Parrinellos's initial study in which they performed electronic structure calculations during the MD simulation (160). This general strategy is gaining more attention for surface and biological reactions because it obviates the need for a functional form. For example, MD simulations of the dissociative chemisorption of a Cl_2 molecule on a 96-atom slab of a $Si\{111\}(2\times1)$ surface using ab initio calculations for the forces have recently been reported (161). The simulation consisted of five trajectories, each of about 0.5 ps duration during which Cl_2 dissociatively chemisorbs on the Si surface (161, 162). They were able to identify active sites for adsorption on the surface. These calculations were performed as part of a Grand Challenge project, and although the computer time is not reported, it is undoubtedly lengthy. Consequently, ab initio MD is not an immediate salvation for large scale simulations at surfaces such as those pictured in Figures 1–3. The large-scale computer simulations of reactions at surfaces, however, are here to stay. The ultimate impact will depend on the availability of better and more diverse many-body PESs. Thus it is a field ripe for more new and creative contributions.

ACKNOWLEDGMENTS

The interest and insight into many-body potentials for reactions at surfaces has come over the years from interactions with many different students, postdocs, and colleagues. In particular we would like to thank MI Baskes, DW Brenner, AE DePristo, FH Stillinger, J Tersoff, JC Tully, V Vitek, and N Winograd for being willing to consult with us and provide information during the past few months. We thank KBS Prasad for the computer graphics and C Moyer for preparing the manuscript. We acknowledge support from the National Science Foundation, the Office of Naval Research, and the IBM-SUR Program. Finally we offer our apologies if we missed some PESs for reactions at surfaces.

Literature Cited

1. Woodruff DP, Delchar TA. 1986. *Modern Techniques of Surface Science*, pp. 435–37. Cambridge: Cambridge Univ. Press
2. Zaera F, Nernstein N. 1994. *J. Am. Chem. Soc.* 116: 4881–87
3. Poon TW, Yip S, Ho PS, Abraham FF. 1990. *Phys. Rev. Lett.* 65: 2161–64
4. Polanyi JC. 1963. *Quant. Spectrosc. Radiat. Transf.* 3: 471–96
5. Polyani JC. 1972. *Acc. Chem. Res.* 5: 161–68
6. Muckerman JT. 1971. *J. Chem. Phys.* 54: 1155–64
7. Muckerman JT. 1972. *J. Chem. Phys.* 56: 2997–3006
8. Muckerman JT. 1972. *J. Chem. Phys.* 57: 3388–96
9. McCreery JH, Wolken G Jr. 1975. *J. Chem. Phys.* 63: 2340–49
10. McCreery JH, Wolken G Jr. 1976. *Chem. Phys. Lett.* 39: 478–80
11. McCreery JH, Wolken G Jr. 1976. *J. Chem. Phys.* 65: 1310–16
12. McCreery JH, Wolken G Jr. 1975. *J. Chem. Phys.* 63: 4072–73
13. McCreery JH, Wolken G Jr. 1976. *J. Chem. Phys.* 64: 2845–53
14. Elkowitz AB, McCreery JH, Wolken G Jr. 1976. *Chem. Phys.* 17: 423–31
15. Gelb A, Cardillo MJ. 1977. *Surf. Sci.* 64: 197–208
16. Andeev VI, Upton TH, Weinberg WH, Goddard WA III. 1980. *Surf. Sci.* 95: 391–402
17. McCreery JH, Wolken G Jr. 1977. *J. Chem. Phys.* 67: 2551–59
18. Gregory AR, Gelb A, Silbey R. 1975. *Surf. Sci.* 74: 497–523
19. Purvis GD III, Wolken G Jr. 1979. *Chem. Phys. Lett.* 62: 42–45
20. Tully JC. 1980. *J. Chem. Phys.* 73: 6333–42
21. Tantardini GF, Simonetta M. 1981. *Surf. Sci.* 105: 517–35
22. Tantardini GF, Simonetta M. 1982. *Chem. Phys. Lett.* 87: 420–25
23. Khanna BC, Saha SH. 1983. *Chem. Phys. Lett.* 95: 217–20
24. Lee C-Y, DePristo AE. 1986. *J. Chem. Phys.* 85: 4161–71
25. Lee C-Y, DePristo AE. 1986. *J. Chem. Phys.* 84: 485–95
26. Truong TN, Hancock G, Truhlar DG. 1989. *Surf. Sci.* 214: 523–59
27. Kara A, DePristo AE. 1987. *Surf. Sci.* 193: 437–54
28. McCreery JH, Wolken G Jr. 1977. *J. Chem. Phys.* 66: 2316–21
29. Lin JH, Garrison BJ. 1984. *J. Chem. Phys.* 80: 2904–13
30. Olson JA, Garrison BJ. 1985. *J. Chem. Phys.* 83: 1392–403
31. Stillinger FH, Weber TA. 1985. *Phys. Rev. B* 31: 5262–71
32. Pearson E, Takai T, Halicioglu T, Tiller WA. 1984. *J. Cryst. Growth* 70: 33–40
33. Axilrod BM, Teller E. 1943. *J. Chem. Phys.* 11: 299–300
34. Tersoff J. 1986. *Phys. Rev. Lett.* 56: 632–35
35. Brenner DW. 1990. *Phys. Rev. B* 42: 9458–71
36. Stillinger FH, Weber TA. 1988. *J. Chem. Phys.* 88: 5123–33
37. Stillinger FH, Weber TA. 1989. *Phys. Rev. Lett.* 62: 2144–47
38. Weber TA, Stillinger FH. 1990. *J. Chem. Phys.* 92: 6239–45
39. Grabow MH, Gilmer GH, Bakker AF. 1989. *Mater. Res. Soc. Proc. Symp.* 141: 349–54
40. Bakker AF, Grabow MH, Gilmer GH, Thompson K. 1990. *J. Comput. Phys.* 90: 313–35
41. Broughton JQ, Li XP. 1987. *Phys. Rev. B* 35: 9120–27
42. Uttormark MJ, Thompson MO, Clancy P. 1993. *Phys. Rev. B* 47: 15717–26
43. Schoolcraft TA, Garrison BJ. 1990. *J. Vac. Sci. Technol. A* 8: 3496–511
44. Schoolcraft TA, Garrison BJ. 1991. *J. Am. Chem. Soc.* 113: 8221–28
45. Walsh R. 1981. *Acc. Chem. Res.* 14: 246–52
46. Ding K, Andersen HC. 1986. *Phys. Rev. B* 34: 6987–91
47. Roland C, Gilmer GH. 1993. *Phys. Rev. B* 47: 16286–98
48. Weakliem PC, Wu CJ, Carter EA. 1992. *Phys. Rev. Lett.* 69: 200–3; Erratum p. 1475
49. Weakliem PC, Carter EA. 1993. *J. Chem. Phys.* 98: 737–45
50. Feil H, Dieleman J, Garrison BJ. 1993. *J. Appl. Phys.* 74: 1303–9
51. Wu CJ, Ionova IV, Carter EA. 1994. *Phys. Rev. B* 49: 13488–500
52. Feurston BP, Garofalini SH. 1988. *J. Chem. Phys.* 89: 5818–24
53. Mahon P, Pailthorpe BA, Bacskay GB. 1991. *Philos. Mag. B* 63: 1419–30
54. Abell GC. 1985. *Phys. Rev. B* 31: 6184–95
55. Tersoff J. 1988. *Phys. Rev. B* 37: 6991–7000
56. Dodson BW. 1987. *Phys. Rev. B* 35: 2795–98
57. Tersoff J. 1988. *Phys. Rev. B* 38: 9902–5

58. Yin MT, Cohen ML. 1983. *Phys. Rev. Lett.* 50: 2006–9
59. Yin MT, Cohen ML. 1984. *Phys. Rev. B* 29: 6996–98
60. Kitabatake M, Fons P, Greene JE. 1990. *J. Vac. Sci. Technol. A* 8: 3726–35
61. Kitabatake M, Fons P, Greene JE. 1991. *J. Vac. Sci. Technol. A* 9: 91–97
62. Kitabatake M, Deguchi M, Hirao T. 1993. *J. Appl. Phys.* 74: 4438–45
63. Srivastava D, Garrison BJ, Brenner DW. 1989. *Phys. Rev. Lett.* 63: 302–5
64. Kelires PC, Tersoff J. 1989. *Phys. Rev. Lett.* 63: 1164–67
65. Tersoff J. 1989. *Phys. Rev. B* 39: 5566–68
66. Wang J, Rockett A. 1991. *Phys. Rev. B* 43: 12571–79
67. Bolding BC, Andersen HC. 1990. *Phys. Rev. B* 41: 10568–85
68. Smith R. 1992. *Nucl. Instrum. Methods Phys. Res. B* 67: 335–39
69. Brenner DW. 1989. *Mater. Res. Soc. Symp. Proc.* 141: 59–64
70. Murty MVR, Atwater HA. 1995. *Phys. Rev. B* 51: 4889–93
71. Khor KE, Das Sarma S. 1988. *Phys. Rev. B* 38: 3318–22
72. Ito T, Khor KE, Das Sarma S. 1989. *Phys. Rev. B* 40: 9715–22
73. Ito T, Khor KE, Das Sarma S. 1989. *Phys. Rev. B* 41: 3893–96
74. Brenner DW, Harrison JA, White CT, Colton RJ. 1991. *Thin Solid Films* 206: 220–23
75. Brenner DW, Robertson DH, Carty RJ, Srivastava D, Garrison BJ. 1992. *Mater. Res. Soc. Meet. Symp. Proc.* 278: 255–60
76. Mowrey RC, Brenner DW, Dunlap BI, Mintmire JW, White CT. 1991. *J. Phys. Chem.* 95: 7138–42
77. Harrison JA, Brenner DW. 1994. *J. Am. Chem. Soc.* 116: 10399–402
78. Garrison BJ, Dawnkaski EJ, Srivastava D, Brenner DW. 1992. *Science* 255: 835–38
79. Taylor RS, Garrison BJ. 1995. *Langmuir.* 11: 1220–28
80. Taylor RS, Garrison BJ. 1994. *J. Am. Chem. Soc.* 116: 4465–66
81. Taylor RS, Garrison BJ. 1994. *Chem. Phys. Lett.* 230: 495–500
82. Peploski J, Thompson DL, Raff LM. 1992. *J. Phys. Chem.* 96: 8538–44
83. Chang X, Perry MD, Peploski J, Thompson DL, Raff LM. 1993. *J. Chem. Phys.* 99: 4748–58
84. Perry MD, Raff LM. 1994. *J. Phys. Chem.* 98: 4375–81
85. Vásquez M, Némethy G, Scheraga HA. 1994. *Chem. Rev.* 94: 2183–239
86. Bareman JP, Cardini G, Klein ML. 1988. *Phys. Rev. Lett.* 60: 2152–55
87. Biswas R, Hamann DR. 1985. *Phys. Rev. Lett.* 55: 2001–4
88. Biswas R, Hamann DR. 1987. *Phys. Rev. B* 36: 6434–45
89. Kwon I, Biswas R, Soukoulis CM. 1992. *Phys. Rev. B* 45: 3332–39
90. Brenner DW, Garrison BJ. 1986. *Phys. Rev. B* 34: 1304–7
91. Keating PN. 1966. *Phys. Rev.* 145: 637–45
92. Baskes MI. 1987. *Phys. Rev. Lett.* 59: 2666–69
93. Kaxiras E, Pandey KC. 1988. *Phys. Rev. B* 38: 12736–39
94. Mistriotis AD, Flytzanis N, Farantos SC. 1989. *Phys. Rev. B* 39: 1212–18
95. Takai T, Halicioglu T, Tiller WA. 1985. *Surf. Sci.* 164: 341–52
96. Takai T, Choi DK, Thathachari YT, Halicioglu T, Tiller WA. 1990. *Phys. Status Solidi B* 157: K13–18
97. Takai T, Lee C, Halicioglu T, Tiller WA. 1990. *J. Phys. Chem.* 94: 4480–82
98. Takai T, Halicioglu T, Tiller WA. 1990. *Phys. Status Solidi B* 157: K77–82
99. Erkoc S, Halicioglu T, Tiller WA. 1992. *Surf. Sci.* 274: 359–62
100. Chelikowsky JR, Phillips JC, Kamal M, Strauss M. 1989. *Phys. Rev. Lett.* 62: 292–95
101. Chelikowsky JR, Phillips JC. 1990. *Phys. Rev. B* 41: 5735–45
102. Chelikowsky JR. 1991. *Phys. Rev. Lett.* 67: 2970–73
103. Murrell JN, Mottram RE. 1990. *Mol. Phys.* 69: 571–85
104. Murrell JN, Rodriguez-Ruiz JA. 1990. *Mol. Phys.* 71: 823–34
105. Al-Derzi AR, Johnston RL, Murrell JN, Rodriguez-Ruiz JA. 1991. *Mol. Phys.* 73: 265–82
106. Eggen BR, Johnston RL, Li S, Murrell JN. 1992. *Mol. Phys.* 76: 619–33
107. Balamane H, Halicioglu T, Tiller WA. 1992. *Phys. Rev. B* 46: 2250–78
108. Cook SJ, Clancy P. 1993. *Phys. Rev. B* 47: 7687–99
109. Ashcroft NW, Mermin ND. 1976. *Solid State Physics.* New York: Holt, Rinehart & Winston
110. Daw MS, Baskes MI. 1983. *Phys. Rev. Lett.* 50: 1285–88
111. Daw MS, Baskes MI. 1984. *Phys. Rev. B* 29: 6443–53
112. Foiles SM, Baskes MI, Daw MS. 1986. *Phys. Rev. B* 33: 7983–92
113. Stott MJ, Zaremba E. 1980. *Phys. Rev. B* 22: 1564–83
114. Nørskov JK, Lang ND. 1980. *Phys. Rev. B* 21: 2131–36

115. Nørskov JK. 1982. *Phys. Rev. B* 26: 2875–85
116. Rose JH, Smith JR, Guinea F, Ferrante J. 1984. *Phys. Rev. B* 29: 2963–69
117. Baskes MI. 1992. *Phys. Rev. B* 46: 2727–42
118. Baskes MI, Johnson RA. 1994. *Model. Simul. Mater. Sci. Eng.* 2: 147–63
119. Foiles SM. 1987. *Surf. Sci.* 191: L779–86
120. Voter AF, Chen SP. 1987. *Mater. Res. Soc. Symp. Proc.* 82: 175–80
121. Voter AF. 1987. *SPIE* 821: 214–26
122. Chen SP, Voter AF, Srolovitz DJ. 1986. *Scr. Metall.* 20: 1389–94
123. Ting N, Qingliang Y, Yiying Y. 1988. *Surf. Sci.* 206: L857–63
124. Garrison BJ, Winograd N, Deaven DM, Reimann CT, Lo DY, et al. 1988. *Phys. Rev. B* 37: 7197–204
125. Ercolessi F, Tosatti E, Parrinello M. 1986. *Phys. Rev. Lett.* 57: 719–22
126. Lim HS, Ong CK, Ercolessi F. 1992. *Surf. Sci.* 269/270: 1109–15
127. Johnson RA. 1988. *Phys. Rev. B* 37: 3924–31
128. Johnson RA. 1989. *Phys. Rev. B* 39: 12554–59
129. Jacobsen KW, Nørskov JK, Puska MJ. 1987. *Phys. Rev. B* 35: 7423–42
130. Stave MS, Sanders DE, Raeker TJ, DePristo AE. 1990. *J. Chem. Phys.* 93: 4413–26
131. Raeker TJ, DePristo AE. 1991. *Int. Rev. Phys. Chem.* 10: 1–54
132. Kelchner CL, Halstead DM, Perkins LS, Wallace NM, DePristo AE. 1994. *Surf. Sci.* 310: 425–35
132a. Rosencrance SW, Burnham JS, Sanders DE, Postawa Z, He C, et al. 1995. *Phys. Rev. B.* In press
133. Raeker TJ, Sanders DE, DePristo AE. 1990. *J. Vac. Sci. Technol. A* 8: 3531–36
134. Raeker TJ, DePristo AE. 1991. *Surf. Sci.* 248: 134–46
135. Schmitz PJ, Leung W-Y, Graham GW, Thiel PA. 1989. *Phys. Rev. B* 40: 11477–87
136. Daw MS, Foiles SM, Baskes MI. 1993. *Mater. Sci. Rep.* 9: 251–310
137. Finnis MW, Sinclair JE. 1984. *Philos. Mag. A* 50: 45–55; Erratum 1986. *Philos. Mag. A* 53: 161
138. Rebonato R, Welch DO, Hatcher RD, Bilello JC. 1987. *Philos. Mag. A* 55: 655–57
139. Ackland GJ, Thetford R. 1987. *Philos. Mag. A* 56: 15–30
140. Eridon J, Rao S. 1989. *Philos. Mag. Lett.* 59: 31–35
141. Johnson RA, Oh DJ. 1989. *J. Mater. Res.* 4: 1195–201
142. Carlsson AE. 1991. *Phys. Rev. B* 44: 6590–97
143. Fang J-Y, Johnston RL, Murrell JN. 1993. *Mol. Phys.* 78: 1405–22
144. Bacon DJ. 1988. *J. Nucl. Mater.* 159: 176–89
145. Oh DJ, Johnson RA. 1989. See Ref. 156, pp. 233–38
146. Oh DJ, Johnson RA. 1989. *J. Mater. Res.* 3: 471–78
147. Igarashi M, Khantha M, Vitek V. 1991. *Philos. Mag. B* 63: 603–27
148. Vitek V, Srolovitz D, eds. 1989. *Atomistic Simulations of Materials: Beyond Pair Potentials.* New York: Plenum
149. Baskes MI, Nelson JS, Wright AF. 1989. *Phys. Rev. B* 40: 6085–100
150. Adams JB, Foiles SM. 1990. *Phys. Rev. B* 41: 3316–28
151. Brenner DW. 1989. *Phys. Rev. Lett.* 63: 1022
152. Ashu P, Matthai CC, Shen T-H. 1991. *Surf. Sci.* 251/252: 955–59
153. Truong TN, Truhlar DG, Garrett BC. 1989. *J. Phys. Chem.* 93: 8227–39
154. Truong TN, Truhlar DG. 1990. *J. Phys. Chem.* 94: 8262–79
155. Kress JD, Voter AF. 1991. *Phys. Rev. B* 43: 12607–10
156. Taylor RS, Brummel CL, Winograd N, Garrison BJ, Vickerman JC. 1995. *Chem. Phys. Lett.* 233: 575–79
157. Taylor RS, Garrison BJ. 1995. *Int. J. Mass Spectrosc. Ion Proc.* 143: 225–33
158. Allinger NL, Yuh YH, Lii J-H. 1989. *J. Am. Chem. Soc.* 111: 8551–75
159. Brummel CL, Lee INW, Zhou Y, Benkovic SJ, Winograd N. 1994. *Science* 264: 399–402
160. Car R, Parrinello M. 1985. *Phys. Rev. Lett.* 55: 2471–74
161. De Vita A, Štich I, Gillan MJ, Payne MC, Clarke LJ. 1993. *Phys. Rev. Lett.* 71: 1276–79
162. Štich I, De Vita A, Payne MC, Gillan MJ, Clarke LJ. 1994. *Phys. Rev. B* 49: 8076–85